Ultrasonics 69 (2016) 144–151

Contents lists available at ScienceDirect

Ultrasonics

journal homepage: www.elsevier.com/locate/ultras

Monte Carlo uncertainty assessment of ultrasonic beam parameters from immersion transducers used to non-destructive testing

A.V. Alvarenga *, C.E.R. Silva, R.P.B. Costa-Félix

Laboratory of Ultrasound/National Institute of Metrology, Quality and Technology, Nossa Senhora das Graças Ave. 50, Duque de Caxias, 25250-020 Rio de Janeiro, Brazil

ARTICLE INFO

Article history:
Received 16 September 2015
Received in revised form 28 January 2016
Accepted 10 April 2016
Available online 11 April 2016

Keywords:
Uncertainty
Ultrasound beam parameters
Non-destructive testing
GUM
Monte Carlo Method

ABSTRACT

The uncertainty of ultrasonic beam parameters from non-destructive testing immersion probes was evaluated using the Guide to the expression of uncertainty in measurement (GUM) uncertainty framework and Monte Carlo Method simulation. The calculated parameters such as focal distance, focal length, focal widths and beam divergence were determined according to EN 12668-2. The typical system configuration used during the mapping acquisition comprises a personal computer connected to an oscilloscope, a signal generator, axes movement controllers, and a water bath. The positioning system allows moving the transducer (or hydrophone) in the water bath. To integrate all system components, a program was developed to allow controlling all the axes, acquire waterborne signals, and calculate essential parameters to assess and calibrate US transducers. All parameters were calculated directly from the raster scans of axial and transversal beam profiles, except beam divergence. Hence, the positioning system resolution and the step size are principal source of uncertainty. Monte Carlo Method simulations were performed by another program that generates pseudo-random samples for the distributions of the involved quantities. In all cases, there were found statistical differences between Monte Carlo and GUM methods.

1. Introduction

When reporting measurement result of a physical quantity, some quantitative indication of the quality of the result shall be given, to allow assessing its reliability. The "Guide to the expression of uncertainty in measurement" (GUM) [1] provides general guidance on many aspects of uncertainty evaluation, as a framework for the uncertainty propagation and the stages of uncertainty evaluation. The GUM uncertainty framework has been adopted by many organizations, is widely used, and has been implemented in standards, guides on measurement uncertainty and in software [1]. However, the GUM approach presents some limitations or drawbacks, as reported in the GUM itself. For instance, the characterization of the output quantity by a Gaussian distribution or a scaled and shifted *t*-distribution, and the restriction of using first-order Taylor series expansion, when the functional relationship between output quantity and its input quantities is nonlinear. Owing such presented limitations, the GUM points out to other analytical or numerical methods [1], such as Monte Carlo Method (MCM).

The Bureau International des *Poids et Mesures* (BIPM) has published the GUM-S1: "Evaluation of measurement data — Supplement 1 to the Guide to the expression of uncertainty in measurement — Propagation of distributions using a Monte Carlo Method" [2] that provides guidelines for the use of MCM, which can be applied to evaluate measurement uncertainties using the concept of propagation of distributions. This concept constitutes a generalization of the law of propagation of uncertainties given by the GUM uncertainty framework. MCM has attracted interest as an alternative method for the evaluation of measurement uncertainties, once MCM can overcome the limitations of the traditional GUM. MCM uses random number generation to simulate values of the involved variables rather than performing analytical calculations. Moreover, MCM approach allows easily taken into account non-linearity in measurement model [2].

Many works in literature have developed and assessed simulations of ultrasonic Non-Destructive Testing (NDT) for evaluating performances of inspection techniques [3–6]. Moreover, the use of realistic data as input parameters for NDT numerical models has also been evaluated [5,7]. However, few of them have presented any concern about measurement uncertainty and its impact on the results of numerical model simulation [5,7], and none even mention the GUM.

Ultrasonic probes play a key role in any ultrasonic measurement system since they both generate and receive the ultrasonic waves. To quantitatively describe the effect of the probe(s) on measured signals during an ultrasonic test, it is necessary to

* Corresponding author.
E-mail addresses: avalvarenga@inmetro.gov.br (A.V. Alvarenga), cesilva@inmetro.gov.br (C.E.R. Silva), rpfelix@inmetro.gov.br (R.P.B. Costa-Félix).

http://dx.doi.org/10.1016/j.ultras.2016.04.009
0041-624X/

characterize both the transducers' transmitting and receiving properties. Despite the fact the beam pattern of an ultrasonic transducer can be theoretically predicted, ultrasonic probe's behaviour can varies from one unit to other, due mostly to their assembly. Because of that, final users should have the most important parameters of ultrasonic probes determined experimentally instead of just consider theoretical formulations [8]. Moreover, it is important to have in mind that the determination of the probe parameters is essential to assess if the ultrasonic probes comply with reference standards, which is intent to assure the quality of probes. According to EN 12668-2 Non-Destructive Testing – Characterization and Verification of Ultrasonic Examination Equipment – Part 2: Probes [9], the beam parameters of immersion ultrasonic probes shall be measured in water and shall comply with their respective acceptance criteria. Besides, those parameters should be verified during the probe's lifetime in order to check if the probe is still adequate to what it was manufactured for. If the beam parameters are determined without estimating their respective measurement uncertainties, the compliance to the acceptance criteria is not properly performed [8].

Inmetro's Laboratory of Ultrasound has developed a measurement system to assess beam parameters of immersion probes and their respective uncertainties, in the frequency range of 0.5 MHz to 10 MHz [10], in accordance with item 7.7 of EN 12668-2 Non-Destructive Testing – Characterization and Verification of Ultrasonic Examination Equipment – Part 2: Probes [9]. To validate the results of the uncertainty calculated according GUM uncertainty framework, the uncertainty using MCM was also calculated. This paper presents the calculation of ultrasonic beam parameters (focal distance, focal length, focal widths and beam divergence) from NDT immersion probes, and its uncertainty evaluation using GUM uncertainty framework and Monte Carlo Method.

2. Beam parameters for immersion probes from EN 12668-2:2010

Immersion probes are specifically designed to transmit ultrasound in applications where the test parts are partially or wholly immersed in water. The relevant beam parameters, as described within this paper, are to be used as defined and assessed, as the beam is formed in water prior to reach the material to be inspected. The measurement procedure used in this paper applies only for those probes. For other types, for instance those generically named "contact probe", there are other approaches to assess its beam parameters, using electromagnetic-acoustic receivers and reference blocks.

Testing beam parameters for immersion probes applied in nondestructive testing is defined in EN 12668-2:2010 standard [9], specifically in the 7.7 subtitle – Beam parameters for immersion probes. Basically, the measurement technique consists at studying the probe ultrasonic beam in water, using a hydrophone receiver. Parameters should be determined by scanning the immersion probe as follows: axial profile (focal distance and length of the focal zone), transverse profile (focal width) at X and Y directions, as well as beam divergence.

Considering V_p as the signal amplitude at the last maximum over the beam axis, the focal distance F_D is given as:

$$F_D = |Z_P - Z_0|, \tag{1}$$

in which Z_P is the position of V_P and Z_0 is the position of the probe face or its acoustic lens (focused probe) (Fig. 1a). For simplicity, assuming $Z_0 = 0$, then $F_D = Z_P$.

The focal length is given by:

$$F_L = |Z_{L2} - Z_{L1}|, \tag{2}$$

in which Z_{L1} and Z_{L2} are the beam axis positions where V_P is reduced by 3 dB (Fig. 1b).

The focal widths on X-axis (W_{x1}) and Y-axis (W_{y1}) at focal point (F_D) are given by the differences:

$$W_{x1} = |X_2 - X_1| \text{ and} \tag{3}$$

$$W_{y1} = |Y_2 - Y_1|, \tag{4}$$

in which X_1 and X_2 (Y_1 and Y_2) are the X (Y) transverse axis positions where V_P is reduced by 3 dB (Fig. 2a). Similarly, the focal widths on X-axis (W_{x2}) and Y-axis (W_{y2}) at Z_{L2} are given by:

$$W_{x2} = |X_{2\_2} - X_{1\_2}| \text{ and} \tag{5}$$

$$W_{y2} = |Y_{2\_2} - Y_{1\_2}|, \tag{6}$$

in which X_{1_2} and X_{2_2} (Y_{1_2} and Y_{2_2}) are the X (Y) transverse axis positions where V_P is reduced by 3 dB (Fig. 2b).

The beam divergence is only required for non-focused probes, therefore excluding those with focusing means, such as acoustic lens or curved piezoelectric elements. Beam divergence parameters are evaluated after the measurement of focal width on F_D and Z_{L2}, as given in (7) and (8):

$$\Omega_x = \frac{360}{2\pi}\arctan\left[\frac{(W_{x2} - W_{x1})}{2(Z_{L2} - F_D)}\right], \tag{7}$$

$$\Omega_y = \frac{360}{2\pi}\arctan\left[\frac{(W_{y2} - W_{y1})}{2(Z_{L2} - F_D)}\right], \tag{8}$$

in which W_{x2} and W_{y2} are the focal width determined on X-axis and Y-axis on Z_{L2} position.

According to EN 12668-2:2010 [9], focal distance, focal length, and focal widths shall be within ±15 % of the manufacturer's specifications, whereas the divergence angles shall not differ from values declared by the manufacture by either ±10% or ±1°, whichever is the largest. It is worth to emphasise that these acceptance criteria are not considered in this study.

3. Measurement system and procedure

The typical system configuration used during the mapping acquisition (Fig. 3) comprises a personal computer connected to an oscilloscope, a signal generator, a needle hydrophone as receiver, and axes movement controllers [10]. A water bath with dimensions of 1700 mm × 1000 mm × 800 mm was used. The positioning system (Newport Corporation, Irvine, CA, USA) comprises X, Y and Z axes movement, and it allows moving the transducer (or hydrophone) in the water bath. The X and Y-axes present accuracy and repeatability better than 1.25 μm, whilst Z achieves a maximum of 5.0 μm in positioning accuracy. Additionally, there is a 360° rotation system, with a 0.01° resolution. To integrate all system components, and also to provide a user-friendly interface, a virtual instrument (VI) was developed in LabVIEW® (National Instruments Corporation, Austin, TX, USA) [11]. The VI allows movement control along all the axes, acquisition of waterborne signals, and the calculation of essential parameters to assess and calibrate US transducers. In addition, the software was developed to automatically perform the raster scans necessary to calculate the immersion probes beam parameters as described in EN 12668-2:2010 [9].

The tests were performed using 10 different NDT ultrasonic unfocused probes varying from 0.5 MHz to 10 MHz nominal frequencies. All probes have 12.7 mm of nominal diameter, except 0.5 MHz frequency probe with 25.4 mm of nominal diameter (Panametrics, Olympus-NDT, USA).

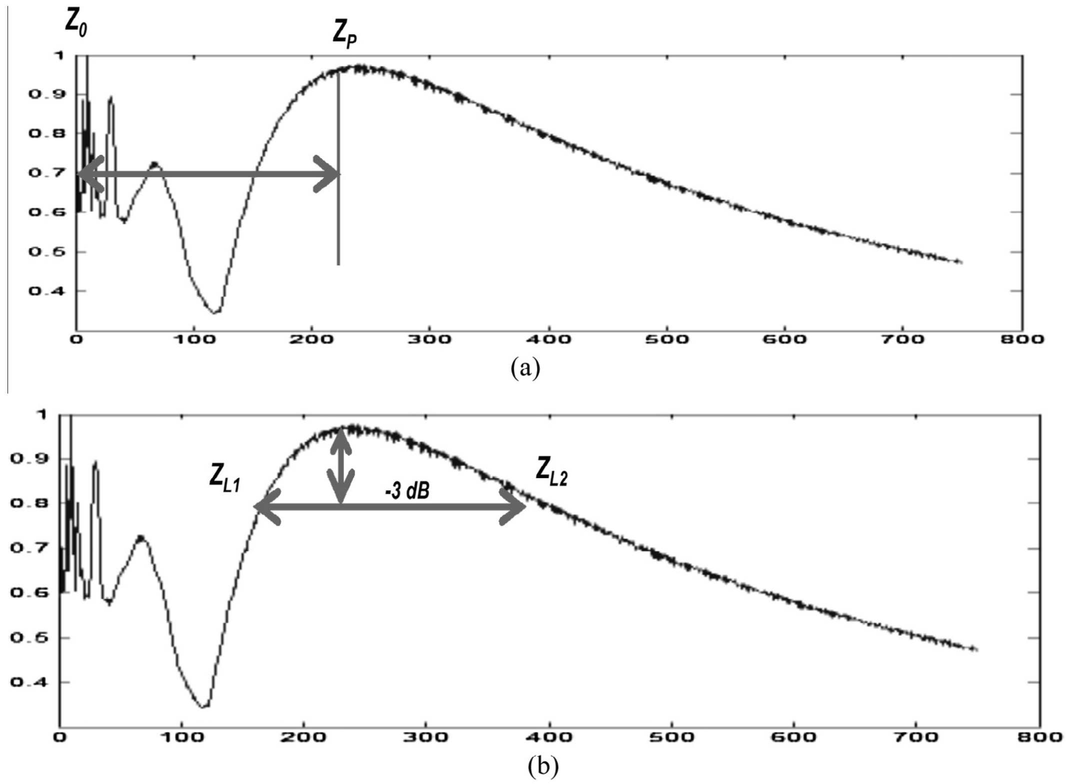

Fig. 1. Example of the positions of (a) Z_P, and (b) Z_{L1} and Z_{L2} over a beam axis profile.

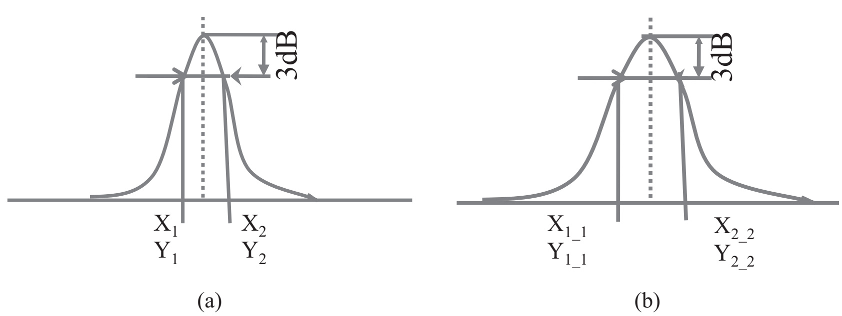

Fig. 2. Example of the transverse axis positions (a) X_1 and X_2 (Y_1 and Y_2) and (b) X_{1_2} and X_{2_2} (Y_{1_2} and Y_{2_2}) over the transverse beam profile.

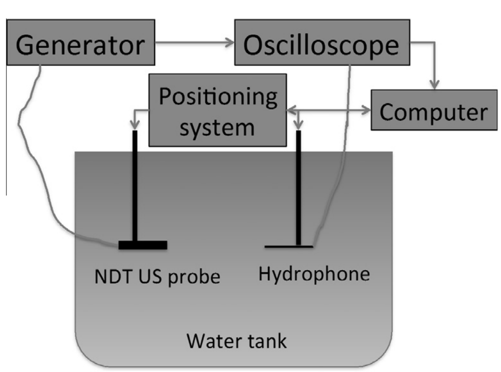

Fig. 3. Block diagram of the experimental setup.

The probes up to 5 MHz were excited by using a 30-cycle sine wave burst, while the probes of 7.5 MHz and 10 MHz were excited by using a 100-cycle sine wave burst, both generated by a function generator model AFG 3252 (Tektronix, Beaverton, Oregon, USA). The water-borne signals were acquired using a needle hydrophone with active element of 0.5 mm (Precision Acoustics Ltd, Dorchester, Dorset, UK) and an oscilloscope TDS 3032B (Tektronix, Beaverton, OR, USA). More details about the measurement can be found in [8].

The theoretical basis of ultrasound propagation shows that the beam parameters are frequency dependent, as for example the focal distance and on-axis pressure distribution [12]. In NDT applications, the centre frequency for a determined probe is used, typically as declared by the manufacturer. In order to reproduce the regular practice in the present work, all experiments were conducted only in the centre frequency of the transducer as defined in its datasheet.

4. Type A and Type B standard uncertainties

As previously presented, all parameters are calculated directly from the raster scans of axial and transversal beam profiles, except beam divergence. Hence, the positioning system resolution (*sp*) and the step size (s) are source of uncertainties to F_D, F_L, Z_{L1}, Z_{L2}, W_{x1}, W_{x2}, W_{y1} and W_{y2}. The positioning system, which performs discrete steps during the raster scan of the ultrasonic beam, has a finite resolution (1.25×10^{-3} mm). According to GUM [1], if the resolution of an instrument is δ_x, the Type B evaluation of standard uncertainty of an instrument can be estimated by a rectangular (uniform) probability distribution of width δ_x with variance $u^2 = \delta_x^2/12$. Hence, the Type B uncertainty of the positioning system is calculated by dividing 1.25×10^{-3} mm by $2\sqrt{3}$. Considering the step size as also presenting a uniform distribution, its Type B uncertainty is defined dividing the actual step size length (0.5 mm or 1 mm) by $2\sqrt{3}$.

As stated in [1], for an input quantity determined from n independent repeated observations, the Type A evaluation of standard uncertainty can be estimated by the experimental standard deviation of the mean. Hence, the Type A standard uncertainty to F_D, F_L, Z_{L1}, Z_{L2}, W_{x1}, W_{x2}, W_{y1} and W_{y2} is evaluated as the standard deviation from 4 repeated measurements divided by $\sqrt{4}$, and the t-distribution is assumed [1]. The number of four repetitions was defined to estimate an uncertainty as close as possible to the practical use of the device under calibration. A larger number of repetitions could produce an artificial assessment of the uncertainty. Finally, the Ω_x and Ω_y uncertainties take into account uncertainties obtained from each one of parameters used in beam divergence calculation.

As stated in [9], in order to guarantee the same sensitivity during a complete measurement, the same hydrophone shall be used for all the beam parameter measurements associated with one particular probe. Hence, in practice, the absolute values of the acoustic pressure are not required as the analysis of measured data is based on relative hydrophone measurements. According to our experience, it is important assess the linearity of the combination among the transducer, the hydrophone and the voltage detection system, in case where corrections shall be made to the measured data [11]. Herein, that combination was assessed to each transducer used in this study, varying input the voltage amplitude and assessing the output voltage. Details about the procedure used here can be found in [11]. The analysis indicates high linearity to all transducers studied ($R > 0.99$), the uncertainty concerning this analysis was negligible ($<10^{-5}$), and no corrections were necessary.

5. Derivation of beam parameter models

Accordingly to [1], for a generic relation $h = f(x_{1,}, \cdots, x_N)$ with no correlation among quantities, the general formula to be used in the uncertainty model is:

$$u_c^2 = \sum_{j=1}^{N} \left(\frac{\partial h}{\partial x_j}\right)^2 \cdot u_j^2 \tag{9}$$

in which u_c is the combined standard uncertainty associated to the final result of measurement (or calculus) of h, and u_j is a standard uncertainty, assessed as Type A or Type B, associated to each parameter or variable x_j used to express the value of h. This model is to be applied to the equation used to completely define the measurand.

Uncertainty for F_D. As previously presented, F_D is determined as the last maximum position of ultrasound beam obtained from the raster scan over the probe axial beam, which means $F_D = Z_P$. The uncertainty of F_D is evaluated from the positioning system ($u_{sp(Type\ B)}$), the step size ($u_{s(Type\ B)}$) and the number of measurements performed ($u_{F_D(Type\ A)}$), as:

$$u_{F_D}^2 = u_{sp(Type\ B)}^2 + u_{s(Type\ B)}^2 + u_{F_D(Type\ A)}^2 \tag{10}$$

Uncertainty for F_L. Considering $Z_{L2} > Z_{L1}$, the sensitivity coefficients for calculating F_L uncertainty are obtained from partial derivatives of Eq. (2):

$$C_{Z_{L2}} = \frac{\partial F_L}{\partial Z_{L2}} = 1, \tag{11}$$

$$C_{Z_{L1}} = \frac{\partial F_L}{\partial Z_{L1}} = -1. \tag{12}$$

Type B uncertainties for Z_{L2} ($u_{Z_{L2}(Type\ B)}$) and Z_{L1} ($u_{Z_{L1}(Type\ B)}$) are defined as the combination of uncertainties from the positioning system ($u_{sp(Type\ B)}$) and the step size ($u_{s(Type\ B)}$), and F_L Type A uncertainty ($u_{F_L(Type\ A)}$) is defined as the standard deviation from the results obtained among the 4 repeated measurements, divided by $\sqrt{4}$. Hence, the F_L combined uncertainty is expressed as:

$$\begin{aligned} u_{F_L}^2 &= c_{Z_{L2}}^2 u_{Z_{L2}(Type\ B)}^2 + c_{Z_{L1}}^2 u_{Z_{L1}(Type\ B)}^2 + u_{F_L(Type\ A)}^2 \\ \therefore u_{F_L}^2 &= u_{Z_{L2}(Type\ B)}^2 + u_{Z_{L1}(Type\ B)}^2 + u_{F_L(Type\ A)}^2 \end{aligned} \tag{13}$$

Uncertainties for W_{x1}, W_{x2}, W_{y1} and W_{y2}. As the calculation models of W are equal, it will be developed the uncertainty model to W_{x1}, only. The uncertainty model for other W can be obtained by analogy. Thus, considering $X_2 > X_1$ and deriving partly Eq. (3), one can obtain the following sensitivity coefficients:

$$C_{W_1\_X_1} = \frac{\partial W_{X1}}{\partial X_1} = 1, \tag{14}$$

$$C_{W_1\_X_2} = \frac{\partial W_{X1}}{\partial X_2} = 1. \tag{15}$$

The uncertainty of W_{x1}, and, by analogy, W_{x2}, W_{y1} and W_{y2} are:

$$u_{W_{x1}}^2 = u_{X_1(Type\ B)}^2 + u_{X_2(Type\ B)}^2 + u_{W_{x1}(Type\ A)}^2 \tag{16}$$

Type B uncertainties are defined as the combination of uncertainties from the positioning system ($u_{sp(Type\ B)}$) and the step size ($u_{s(Type\ B)}$), and Type A uncertainties are defined from the results obtained among the 4 repeated measurements, divided by $\sqrt{4}$.

Uncertainties for Ω_x and Ω_y. The sensitivity coefficients for calculating Ω_x uncertainty (and by analogy Ω_y) are obtained from partial derivatives of Eq. (7) (and (8) by analogy):

$$c_{\Omega_x\_W_{x1}} = \frac{\partial \Omega_x}{\partial W_{x1}} = -\frac{1}{(2Z_{L2} - 2F_D) \cdot \left(1 + \frac{(W_{x2}-W_{x1})^2}{(2Z_{L2}-2F_D)^2}\right)}, \tag{17}$$

$$c_{\Omega_x\_W_{x2}} = \frac{\partial \Omega_x}{\partial W_{x2}} = \frac{1}{(2Z_{L2} - 2F_D) \cdot \left(1 + \frac{(W_{x2}-W_{x1})^2}{(2Z_{L2}-2F_D)^2}\right)} \tag{18}$$

$$c_{\Omega_x\_Z_{L2}} = \frac{\partial \Omega_x}{\partial Z_{L2}} = -2 \cdot \frac{W_{x2} - W_{x1}}{(2Z_{L2} - 2F_D) \cdot \left(1 + \frac{(W_{x2}-W_{x1})^2}{(2Z_{L2}-2F_D)^2}\right)} \tag{19}$$

$$c_{\Omega_x\_F_D} = \frac{\partial \Omega_x}{\partial F_D} = 2 \cdot \frac{W_{x2} - W_{x1}}{(2Z_{L2} - 2F_D) \cdot \left(1 + \frac{(W_{x2}-W_{x1})^2}{(2Z_{L2}-2F_D)^2}\right)} \tag{20}$$

Hence, Ω_x (and by analogy Ω_y) combined uncertainty is given by:

$$\begin{aligned} u_{\Omega_x}^2 &= c_{\Omega_x\_W_{x1}}^2 u_{W_{x1}}^2 + c_{\Omega_x\_W_{x2}}^2 u_{W_{x2}}^2 + c_{\Omega_x\_Z_{L2}}^2 (u_{Z_{L2(Type\ A)}}^2 + u_{Z_{L2(Type\ B}}^2) \\ &\quad + c_{\Omega_x\_F_D}^2 u_{F_D}^2 + u_{\Omega_x(Type\ A)}^2 \end{aligned} \tag{21}$$

The respective coverage factors were determined considering a coverage probability of 95% (t-distribution) and the effective degrees of freedom obtained from the Welch–Satterthwaite formula [1]. Examples of uncertainty budget for each one of the studied parameters are presented in Tables 1–4.

Table 1
Example of F_D uncertainty budget for the 1.0 MHz transducer (diameter: 12.7 mm).

Quantity	Estimate	Standard uncertainty	Probability distribution	Sensitivity coefficients	Uncertainty contribution	Degrees of freedom (v_i)	Combined uncertainty (Eq. (8))	v_{eff}	k (95%)	Expanded uncertainty mm	Expanded uncertainty %
Positioning system/mm $u_{sp(Type\ B)}$	1.0	$\frac{1.25\times10^{-3}}{2\sqrt{3}}$	Uniform	1	3.61×10^{-4}	∞	3.82×10^{-1}	22	2.08	0.80	3.0
Step/mm $u_{s(Type\ B)}$	1.0	$\frac{1}{2\sqrt{3}}$	Uniform	1	2.89×10^{-1}	∞					
F_D /mm $u_{F_D(Type\ A)}$	26.25	2.50×10^{-1}	t-distribution	1	2.50×10^{-1}	4					

Table 2
Example of F_L uncertainty budget for the 1.0 MHz transducer (diameter: 12.7 mm).

Quantity	Estimate	Standard uncertainty	Probability distribution	Sensitivity coefficients	Uncertainty contribution	Degrees of freedom (v_i)	Combined uncertainty (Eq. (8))	v_{eff}	k (95%)	Expanded uncertainty mm	Expanded uncertainty %
Z_{L1} /mm $u_{Z_{L1}(Type\ B)}$	16.50	2.89×10^{-1}	Uniform	−1	2.89×10^{-1}	∞	7.50×10^{-1}	8.08	2.31	1.7	4.3
Z_{L2} /mm $u_{Z_{L2}(Type\ B)}$	56.75	2.89×10^{-1}	Uniform	1	2.89×10^{-1}	∞					
F_L /mm $u_{F_L(Type\ A)}$	40.25	4.08×10^{-1}	t-distribution	1	4.08×10^{-1}	4					

Table 3
Example of W_{x1} uncertainty budget for the 1.0 MHz transducer (diameter: 12.7 mm).

Quantity	Estimate	Standard uncertainty	Probability distribution	Sensitivity coefficients	Uncertainty contribution	Degrees of freedom (v_i)	Combined uncertainty (Eq. (8))	v_{eff}	k (95%)	Expanded uncertainty mm	Expanded uncertainty %
X_1/mm $u_{X_1(Type\ B)}$	8.20	2.89×10^{-2}	Uniform	-1	2.89×10^{-2}	∞	6.29×10^{-2}	12	2.20	0.14	3.8
X_2/mm $u_{X_2(Type\ B)}$	11.93	2.89×10^{-2}	Uniform	1	2.89×10^{-2}	∞					
W_{x1}/mm $u_{W_{x1}(Type\ A)}$	3.70	4.79×10^{-2}	t-distribution	1	4.79×10^{-2}	4					

6. Monte Carlo simulation (GUM-S1)

Monte Carlo Method provides a general approach to obtain an approximate numerical representation of the distribution function of a measurand, based on repeated sampling from the input quantities distribution functions and the evaluation of the model in each case. As stated in [2], expectations and variances of the distribution functions can be determined directly from the set of model values obtained. Hence, the input quantities (expectations) used in the Monte Carlo Method were the same ones measured to determine the measurement uncertainty using the GUM framework (Tables 1–4). Correspondingly, the probability distribution and the dispersion values (variances) of those distributions were determined based on the standard uncertainty of each quantity. Considering t-distributions, the standard deviation was defined as the standard uncertainty itself, while the interval of uniform distributions was set as the standard uncertainty multiplied by $2\sqrt{3}$. The only exception is the parameter beam divergence (Eqs. (6) and (7)) that is calculated using the probability distributions of the parameters obtained previously by the Monte Carlo simulation. In this case, the probability distributions described in Table 4 are used only to the GUM framework.

Monte Carlo Method simulations were performed by a program developed in LabVIEW® to generate pseudo random probabilities for the distributions of the involved quantities. Uniform pseudo random numbers were generated using a modified version of the Very-Long-Cycle random number generator algorithm, which produces approximately 2^{90} samples before the pattern repeats itself. In the case of t-distributions, a modified version of the Box-Muller method to transform uniformly distributed random numbers into t-distributed random numbers was used. These algorithms are part of LabVIEW® Signal Generation VIs palette. Hence, 1×10^9 possible random values were generated for each quantity that were performed by accumulation of the data from 2000 single simulations with 5×10^5 trials each, according to their distribution functions, to evaluate studied parameters uncertainties. The endpoints of the coverage interval were on both sides of the output distribution function in the neighbourhood of 2.5% (y_{low}) and 97.5% (y_{high}), respectively.

The validation was performed as indicated in [2], determining whether the coverage intervals obtained by the GUM uncertainty framework, $[y - U_p;\ y + U_p]$, in which y is the estimate and U_p expanded uncertainty, and MCM GUM-S1 ($[y_{\text{low}};\ y_{\text{high}}]$) agree to within a stipulated numerical tolerance (δ), regarded as a meaningful number of significant decimal digits from the standard uncertainty. For details in determining δ, please refer to item 7.9.2 in [2].

7. Results and discussion

The standard uncertainty values evaluated to the studied parameters, using the GUM and MCM (GUM-S1), are presented in Tables 5–10, for transducers of 1 MHz, 2.25 MHz, 3.5 MHz, 5.0 MHz, 7.5 MHz and 10 MHz, respectively. One can observe that the mean values and the combined uncertainties are identical for the following beam parameters: F_D, F_L, Z_{L1}, Z_{L2}, W_{x1}, W_{x2}, W_{y1} and W_{y2}. However, one can observe that probability density functions provided by MCM give shorter coverage intervals than those provided by the GUM uncertainty framework. Considering the beam divergence parameter (Ω_x and Ω_y), the mean values calculated by both approaches are quite similar. Nevertheless, MCM approach gives higher values of combined uncertainties and larger coverage intervals.

Table 4
Example of Ω_x uncertainty budget for the 1.0 MHz transducer (diameter: 12.7 mm).

Quantity	Estimate	Standard uncertainty	Probability distribution	Sensitivity coefficients	Uncertainty contribution	Degrees of freedom (ν_i)	Combined uncertainty (Eq. (8))	ν_{eff}	k (95%)	Expanded uncertainty mm	Expanded uncertainty %
W_{x1}/mm $u_{W_{x1}(Type\ B)}$	3.70	6.29×10^{-2}	t-distribution	-9.37×10^{-1}	-5.89×10^{-2}	∞	1.22×10^{-1}	∞	2	0.25	8.2
W_{x2}/mm $u_{W_{x2}(Type\ B)}$	6.55	6.29×10^{-2}	t-distribution	9.37×10^{-1}	5.89×10^{-2}	∞					
F_D/mm $u_{F_D(Type\ B)}$	60.5	3.82×10^{-1}	t-distribution	-9.98×10^{-2}	-3.81×10^{-2}	∞					
Z_{L2}/mm $u_{Z_{L2}(Type\ B)}$	123	8.04×10^{-1}	t-distribution	-9.98×10^{-2}	-8.02×10^{-2}	∞					
Ω_x/mm $u_{\Omega_x(Type\ A)}$	3.05	1.46×10^{-2}	t-distribution	1	1.46×10^{-2}	4					

Table 5
Comparison between GUM and Monte Carlo simulation (GUM-S1) uncertainty evaluation methods, for the NDT probes 1 (1 MHz – Ø = 12.7 mm).

Quantity	GUM				MCM (GUM-S1)			d_{low}	d_{high}	GUM validated
	Estimate	Standard uncertainty	k	95% coverage interval	Estimate	Standard uncertainty	95% coverage interval			
F_D (mm)	26.25	0.38	2.08	[25.46, 27.04]	26.25	0.38	[25.52, 26.98]	0.06	0.06	No
F_L (mm)	40.25	0.75	2.31	[38.52, 41.98]	40.25	0.75	[38.79, 41.72]	0.27	0.26	No
W_{x1} (mm)	3.725	0.063	2.20	[3.587, 3.863]	3.725	0.063	[3.602, 3.848]	0.02	0.02	No
W_{y1} (mm)	3.70	0.10	2.57	[3.44, 3.96]	3.70	0.10	[3.50, 3.90]	0.06	0.06	No
W_{x2} (mm)	6.975	0.063	2.20	[6.837, 7.110]	6.975	0.063	[6.852, 7.098]	0.02	0.02	No
W_{y2} (mm)	6.950	0.076	2.36	[6.769, 7.131]	6.950	0.076	[6.802, 7.100]	0.03	0.03	No
Ω_x (°)	3.05	0.12	2.00	[2.81, 3.29]	3.05	0.12	[2.82, 3.30]	0.01	0.01	No
Ω_y (°)	3.05	0.15	2.00	[2.76, 3.35]	3.05	0.15	[2.76, 3.35]	0.01	0.00	Yes

Table 6
Comparison between GUM and Monte Carlo simulation (GUM-S1) uncertainty evaluation methods, for the NDT probes 2 (2.25 MHz – Ø = 12.7 mm).

Quantity	GUM				MCM (GUM-S1)			d_{low}	d_{high}	GUM validated
	Estimate	Standard uncertainty	k	95% coverage interval	Estimate	Standard uncertainty	95% coverage interval			
F_D (mm)	63.0	1.0	2.78	[60.1, 65.9]	63.0	1.0	[61.0, 65.1]	0.84	0.84	No
F_L (mm)	93.75	0.48	2.01	[92.79, 94.71]	93.75	0.48	[92.82, 94.68]	0.03	0.03	No
W_{x1} (mm)	3.88	0.11	2.57	[3.59, 4.16]	3.88	0.11	[3.66, 4.09]	0.07	0.07	No
W_{y1} (mm)	3.93	0.13	2.78	[3.56, 4.29]	3.93	0.13	[3.67, 4.18]	0.11	0.11	No
W_{x2} (mm)	7.000	0.082	2.36	[6.807, 7.193]	7.000	0.082	[6.841,7.160]	0.03	0.03	No
W_{y2} (mm)	7.075	0.075	2.31	[6.902, 7.248]	7.075	0.075	[6.929, 7.222]	0.03	0.03	No
Ω_x (°)	1.283	0.060	2.00	[1.163, 1.404]	1.284	0.069	[1.148, 1.421]	0.02	0.02	No
Ω_y (°)	1.293	0.065	2.00	[1.162, 1.424]	1.294	0.074	[1.149, 1.440]	0.01	0.02	No

Table 7
Comparison between GUM and Monte Carlo simulation (GUM-S1) uncertainty evaluation methods, for the NDT probes 3 (3.5 MHz – Ø = 12.7 mm).

Quantity	GUM				MCM (GUM-S1)			d_{low}	d_{high}	GUM validated
	Estimate	Standard uncertainty	k	95% coverage interval	Estimate	Standard uncertainty	95% coverage interval			
F_D (mm)	97.75	0.99	2.78	[95.00, 100.50]	95.75	0.99	[95.81, 99.69]	0.81	0.81	No
F_L (mm)	135.25	0.85	2.45	[133.16, 137.34]	135.25	0.85	[133.58, 136.92]	0.42	0.42	No
W_{x1} (mm)	3.700	0.041	2.00	[3.618, 3.782]	3.700	0.041	[3.623, 3.777]	0.005	0.005	No
W_{y1} (mm)	3.68	0.075	2.31	[3.502, 3.848]	3.675	0.075	[3.528, 3.821]	0.03	0.03	No
W_{x2} (mm)	6.800	0.058	2.13	[6.677, 6.923]	6.800	0.058	[6.688, 6.912]	0.01	0.01	No
W_{y2} (mm)	6.900	0.058	2.12	[6.778, 7.022]	6.900	0.058	[6.788, 7.012]	0.01	0.01	No
Ω_x (°)	0.886	0.023	2.00	[0.839, 0.933]	0.886	0.042	[0.804, 0.968]	0.04	0.04	No
Ω_y (°)	0.921	0.030	2.00	[0.861, 0.981]	0.922	0.046	[0.833, 1.011]	0.03	0.03	No

For all studied parameters, the coverage intervals were compared taking into account the calculation of the numerical tolerance [2], and results point out that they are statistically different. It is important to go deeply in the essence of the GUM model. It is, fundamentally, a simplification, in which all theoretical and statistical assessment is based in normal or t-student distributions. The MCM, on the other hand, starts from the fundamental principle that each parameter distribution may or may not be normal, and whatever the distributions are, the combinations are done with the distributions themselves, and not on simplified expressions of it (as mean values and standard deviations). These differences tend to emerge when a Gaussian distribution cannot approximate the probability distribution function for the output quantity, or the model is non-linear [2]. In the present context, "non-linear" is the behaviour of a parameter's formulae (Eqs. (7) and (8)). For instance, the beam divergence parameter is calculated from an arctan func-

Table 8
Comparison between GUM and Monte Carlo simulation (GUM-S1) uncertainty evaluation methods, for the NDT probes 4 (5 MHz – Ø = 12.7 mm).

Quantity	GUM				MCM (GUM-S1)			d_{low}	d_{high}	GUM validated
	Estimate	Standard uncertainty	k	95% coverage interval	Estimate	Standard uncertainty	95% coverage interval			
F_D (mm)	142.25	0.80	2.57	[140.18, 144.32]	142.25	0.80	[140.67, 143.82]	0.49	0.50	No
F_L (mm)	173.00	0.82	2.36	[171.07, 174.93]	173.00	0.82	[171.4, 174.60]	0.33	0.33	No
W_{x1} (mm)	3.550	0.050	2.03	[3.449, 3.651]	3.550	0.050	[3.453, 3.646]	0.004	0.01	No
W_{y1} (mm)	3.500	0.058	2.12	[3.378, 3.622]	3.5	0.058	[3.388, 3.612]	0.01	0.01	No
W_{x2} (mm)	6.400	0.058	2.13	[6.277, 6.523]	6.400	0.058	[6.288, 6.513]	0.01	0.01	No
W_{y2} (mm)	6.375	0.048	2.01	[6.279, 6.471]	6.375	0.048	[6.283, 6.467]	0.004	0.004	No
Ω_x (°)	0.653	0.018	2.00	[0.617, 0.690]	0.653	0.040	[0.576, 0.730]	0.04	0.04	No
Ω_y (°)	0.659	0.018	2.00	[0.623, 0.695]	0.659	0.040	[0.582, 0.736]	0.04	0.04	No

Table 9
Comparison between GUM and Monte Carlo simulation (GUM-S1) uncertainty evaluation methods, for the NDT probes 5 (7.5 MHz – Ø = 12.7 mm).

Quantity	GUM				MCM (GUM-S1)			d_{low}	d_{high}	GUM validated
	Estimate	Standard uncertainty	k	95% coverage interval	Estimate	Standard uncertainty	95% coverage interval			
F_D (mm)	163.5	2.4	2.78	[156.8, 170.2]	163.5	2.4	[158.8, 168.2]	1.98	1.97	No
F_L (mm)	163.3	1.8	2.78	[158.4, 168.1]	163.3	1.8	[159.8, 166.7]	1.41	1.45	No
W_{x1} (mm)	2.675	0.038	2.36	[2.585, 2.765]	2.675	0.038	[2.600, 2.750]	0.02	0.02	No
W_{y1} (mm)	2.625	0.048	2.57	[2.502, 2.748]	2.625	0.048	[2.531, 2.719]	0.03	0.03	No
W_{x2} (mm)	4.350	0.029	2.13	[4.288, 4.412]	4.350	0.029	[4.294, 4.406]	0.01	0.01	No
W_{y2} (mm)	4.300	0.071	2.78	[4.104, 4.496]	4.300	0.071	[4.162, 4.439]	0.06	0.06	No
Ω_x (°)	0.430	0.011	2.00	[0.409, 0.452]	0.430	0.040	[0.352, 0.508]	0.06	0.06	No
Ω_y (°)	0.430	0.016	2.00	[0.397, 0.462]	0.430	0.044	[0.345, 0.516]	0.05	0.05	No

Table 10
Comparison between GUM and Monte Carlo simulation (GUM-S1) uncertainty evaluation methods, for the NDT probes 6 (10 MHz – Ø = 12.7 mm).

Quantity	GUM				MCM (GUM-S1)			d_{low}	d_{high}	GUM validated
	Estimate	Standard Uncertainty	k	95% coverage interval	Estimate	Standard uncertainty	95% coverage interval			
F_D (mm)	231.3	2.0	2.78	[225.8, 236.7]	231.3	2.0	[227.4, 235.08]	1.60	1.59	No
F_L (mm)	243.3	1.5	2.78	[239.0, 247.5]	243.3	1.6	[240.2, 246.3]	1.25	1.29	No
W_{x1} (mm)	2.825	0.078	2.78	[2.609, 3.041]	2.825	0.078	[2.673, 2.978]	0.06	0.06	No
W_{y1} (mm)	2.875	0.069	2.78	[2.683, 3.067]	2.875	0.069	[2.74, 3.011]	0.06	0.06	No
W_{x2} (mm)	4.125	0.052	2.57	[3.991, 4.259]	4.125	0.052	[4.023, 4.228]	0.03	0.03	No
W_{y2} (mm)	4.138	0.052	2.57	[4.005, 4.270]	4.138	0.051	[4.037, 4.238]	0.03	0.03	No
Ω_x (°)	0.330	0.012	2.00	[0.306, 0.353]	0.330	0.043	[0.246, 0.414]	0.06	0.06	No
Ω_y (°)	0.320	0.011	2.00	[0.298, 0.342]	0.320	0.042	[0.238, 0.403]	0.06	0.06	No

tion, i.e., a non-linear function. There is a very clear difference between an arctan and a t-distribution. Because of that, when applying MCM in the beam divergence parameter, the output distribution and the coverage interval for a given coverage probability tend to differ from the GUM framework model.

In a previous work [8], it was demonstrated that some beam parameter values declared by the manufacturer could be statistically different from the one measured in the laboratory, using the GUM uncertainty framework. Herein, it was shown that MCM would be the suitable approach to assess those parameters and, in some cases, more restrictive coverage intervals were achieved. However, despite of the shorter coverage intervals, the beam parameter values would be accepted considering the EN 12668-2 criteria, which could be considered conservatives.

8. Conclusion

This paper has presented a detailed comparative study between the GUM approach and the MCM approach using GUM Supplement 1 for the uncertainty evaluation of ultrasonic beam parameters (focal distance, focal length, focal widths and beam divergence) from NDT immersion probes. For all studied parameters, the results show that the coverage intervals achieved using GUM and MCM approaches were statistically different, pointing out that the MCM should be used instead of GUM framework uncertainty. This result has a direct consequence on the assessment of ultrasound probes used in non-destructive testing, and their usability according to the international standard EN 12668-2.

The development of the uncertainty framework for the beam parameters of immersion ultrasonic probes is an original approach that can help researchers, manufacturers, or accredited test laboratories with the analysis of their measurements and uncertainty models. Further, the findings disclosed in this paper could be used to improve the standard EN 12668-2 in a future revision, mainly in the definition of a guide to estimate the measurement uncertainty, once the actual edition makes no reference about how the uncertainty could be assessed.

Acknowledgements

The authors would like to acknowledge the financial support from the “Fundação Carlos Chagas Filho de Amparo à Pesquisa do

Estado do Rio de Janeiro" (FAPERJ – Grant Number: E-26/201.563/2014) and to the National Council for Scientific and Technological Development (Grant Numbers: 309717/2014-0 and 310.392/2014-4).

References

[1] BIPM, IEC, IFCC, ILAC, ISO, IUPAC, IUPAP, and OIML, Evaluation of Measurement Data — Guide to the Expression of Uncertainty in Measurement, Joint Committee for Guides in Metrology, JCGM 100, 2008.
[2] BIPM, IEC, IFCC, ILAC, ISO, IUPAC, IUPAP, and OIML, Evaluation of Measurement Data — Supplement 1 to the "Guide to the Expression of Uncertainty in Measurement" — Propagation of Distributions using a Monte Carlo Method, Joint Committee for Guides in Metrology, JCGM 101:2008, 2008.
[3] S. Kolkoori, K. Chitti Venkata, K. Balasubramaniam, Quantitative simulation of ultrasonic time of flight diffraction technique in 2D geometries using Huygens–Fresnel diffraction model: theory and experimental comparison, Ultrasonics 55 (2015) 33–41.
[4] M. Darmon et al., A system model for ultrasonic NDT based on the Physical Theory of Diffraction (PTD), Ultrasonics 64 (2016) 115–127.
[5] M.A. Ploix, P. Guy, B. Chassignole, J. Moysan, G. Corneloup, R. El Guerjouma, Measurement of ultrasonic scattering attenuation in austenitic stainless steel welds: realistic input data for NDT numerical modeling, Ultrasonics 54 (2014) 1729–1736.
[6] S. Chatillon, L. de Roumilly, J. Porre, C. Poidevin, P. Calmon, Simulation and data reconstruction for NDT phased array techniques, Ultrasonics 44 (2006) e951–e955.
[7] F. Rupin, G. Blatman, S. Lacaze, T. Fouquet, B. Chassignole, Probabilistic approaches to compute uncertainty intervals and sensitivity factors of ultrasonic simulations of a weld inspection, Ultrasonics 54 (2014) 1037–1046.
[8] C.E.R. Silva, A.V. Alvarenga, R.P.B. Costa-Félix, Nondestructive testing ultrasonic immersion probe assessment and uncertainty evaluation according to EN 12668–2:2010, IEEE Trans. Ultrason. Ferroelectr. Freq. Control 59 (2012) 2338–2346.
[9] EN 12668-2:2010, Non Destructive Testing – Characterization and Verification of Ultrasonic Examination Equipment – Part 2: Probes (2010).
[10] C.E.R. Silva, A.V. Alvarenga, R.P.B. Costa-Félix, Ultrasonic immersion probes characterization for use in non destructive testing according to EN 12668-2:2001, J. Phys: Conf. Ser. 279 (2010) 1–6.
[11] A.V. Alvarenga, R.P.B. Costa-Félix, Uncertainty assessment of effective radiating area and beam non-uniformity ratio of ultrasound transducers determined according to IEC 61689:2007, Metrologia 46 (2009) 367–374.
[12] P.R. Stepanishen, Transient radiation from pistons in an infinite planar baffle, J. Acoust. Soc. Am. 49 (5 – Part 2) (1971) 1629–1638.